Int. J. Engng Sci. Vol. 26, No. 11, pp. 1177–1187, 1988
Printed in Great Britain.

0020–7225/88 $3.00 + 0.00

EFFECT OF MULTIPLE INITIAL IMPERFECTIONS ON THE INITIATION AND GROWTH OF ADIABATIC SHEAR BANDS IN NONPOLAR AND DIPOLAR MATERIALS

Y. W. KWON and R. C. BATRA

Department of Engineering Mechanics, University of Missouri-Rolla, Rolla, MO 65401-0249, U.S.A.

Abstract—Simple shearing deformations of a viscoplastic block made of nonpolar and dipolar materials, and placed in a hard loading device are studied. Multiple defects in the block are modeled by perturbing the uniform temperature within the block when the material just starts deforming plastically to that given by a cosine function which assumes relative maximum values at several points in the block. It is found that for simple materials, the deformation localizes at points where the perturbed temperature has relative minima when the average applied strain-rate $\dot{\gamma}_0$ is $500\,s^{-1}$ and at the locations of the relative maxima of the perturbed temperature when the applied strain-rate is more than $1000\,s^{-1}$. This transition occurs possibly due to different thermal lengths and the time scales associated with the work-hardening in the two cases. For dipolar materials the deformation localizes near the boundaries of the block abutting the loading device when $\dot{\gamma}_0 = 500\,s^{-1}$ but at the locations of the relative maxima of the perturbed temperature when $\dot{\gamma}_0 = 50{,}000\,s^{-1}$. For both simple and dipolar materials the initiation of the localization of the deformation is considerably delayed as compared to the case when the temperature perturbation has only one bump with its center coinciding with the center of the block.

INTRODUCTION

Recently there has been considerable interest in the study of the localization of the shearing deformation in bodies being deformed at very high strain-rates. These narrow regions of severe deformation are usually referred to as adiabatic shear bands because of the little time available for the heat generated to diffuse away to colder regions of the body. These shear bands are believed to be precursors to shear fractures.

Most analytical studies (e.g. Recht [1], Staker [2], Clifton [3], Burns [4], Bai [5] and Shawki *et al.* [6]), aimed at delineating factors that inhibit or enhance the initiation and growth of adiabatic shear bands, have involved analyzing the thermomechanical deformations of a block undergoing simple shearing deformations. Whereas Recht, Staker and Clifton derived conditions based on the assumption that the material point becomes unstable when the shear stress at that point attains a maximum value, Burns, Bai and Shawki *et al.* studied the growth of small perturbations superimposed on a finitely deformed body. In these latter analytical studies the governing equations were linearized around the finitely deformed state. Clifton *et al.* [7], Wright and Batra [8, 9], Wright and Walter [10] and Batra [11] studied, numerically, the effect of introducing a perturbation on a finitely deformed body and did not need to linearize the governing equations. Subsequently Batra [12] introduced the temperature perturbation when the body just starts deforming plastically and investigated the effect of various material parameters on the value of the average strain at which the deformation begins to localize. These perturbations are supposed to simulate the flaws or inhomogeneities present in the material. Whereas in previous works one or two flaws/defects were presumed to be present, here we assume that the flaws are periodically distributed and represent these by an initial temperature distribution given by a cosine function which assumes relative maximum values at several points in the specimen. It is found that the presence of many flaws/defects delays considerably the initiation of the localization of the deformation.

Wright and Batra [9] and Batra [11] have shown that the inclusion of the strain gradients as an independent kinematic variable has a stiffening effect in the sense that it delays considerably the onset of shear bands. Batra [11] also studied the interaction among shear bands in simple and dipolar materials. His numerical calculations revealed that two bands that will grow independently in simple materials will coalesce in dipolar materials. Herein it is found that in dipolar materials the deformation localizes near the boundaries of the specimen at an applied

strain-rate $\dot{\gamma}_0$ of $500\,s^{-1}$ but at the locations of the relative maxima of the initial temperature when $\dot{\gamma}_0 = 50{,}000\,s^{-1}$. In simple materials the deformation localized at points between the locations of the relative maxima of the initial temperature at $\dot{\gamma}_0 = 500\,s^{-1}$. However, at $\dot{\gamma}_0 = 50{,}000\,s^{-1}$ the points where the deformation localized coincided with the locations of the relative maxima of the initial temperature.

FORMULATION OF THE PROBLEM

Equations governing the thermomechanical deformations of a block occupying the region $-1 \leq y \leq +1$ and made of a viscoplastic material undergoing simple shearing deformations may be written [9, 11] as

$$\dot{v} = \frac{1}{\rho}(s - l\sigma_{,y})_{,y}, \tag{1}$$

$$\dot{\theta} = k\theta_{,yy} + \Lambda(s^2 + \sigma^2), \tag{2}$$

$$\dot{s} = \mu(v_{,y} - \Lambda s), \tag{3}$$

$$\dot{\sigma} = l\mu\left(v_{,yy} - \frac{\Lambda}{l}\sigma\right), \tag{4}$$

$$\dot{\psi} = \Lambda(s^2 + \sigma^2)\Big/\left(1 + \frac{\psi}{\psi_0}\right)^n, \tag{5}$$

$$\Lambda = \max\left\{0, \left[\left(\frac{(s^2+\sigma^2)^{\frac{1}{2}}}{\left(1+\frac{\psi}{\psi_0}\right)^n(1-a\theta)}\right)^{1/m} - 1\right]\Big/\left[b(s^2+\sigma^2)^{1/2}\right]\right\}. \tag{6}$$

These equations are written in terms of nondimensional variables. Equations (1) and (2) represent, respectively, the balance of linear momentum and the balance of internal energy. The balance of mass simply gives that the mass density ρ stays constant since the simple shearing deformation is isochoric. Here v is the x-velocity of a material particle, θ its temperature change from that in the reference configuration, s is the shear stress in the x direction acting on the plane y = constant, σ is the dipolar stress on this plane, k the thermal diffusivity, parameters ψ_0 and n describe the strain-hardening of the material, parameters b and m characterize the strain-rate sensitivity of the material, the parameter a defines the thermal softening, the parameter l is the material characteristic length, and μ is the shear modulus. The parameter ψ may be thought of as an internal variable and eqn (5) its growth equation. It is used to describe the work-hardening of the material. Note that the numerator on the right-hand side of eqn (5) equals the plastic working. A comma followed by y signifies partial differentiation with respect to y and a superimposed dot stands for the material time differentiation. Implicit in eqn (2) are the assumptions that the specific internal energy equals the specific heat multiplied by the change in temperature, Fourier's law of heat conduction holds and that all of the plastic working is converted into heat. The material characteristic length l equals zero for nonpolar materials and is positive for dipolar materials.

In eqns (1)–(6) it has also been assumed that the strain rate $\dot{\gamma} = v_{,y}$ and its gradient $\dot{d} = v_{,yy}$ have additive decompositions into elastic $\dot{\gamma}_e$, $\dot{d}_e$ and plastic parts $\dot{\gamma}_p$, $\dot{d}_p$. That is

$$\dot{\gamma} = \dot{\gamma}_e + \dot{\gamma}_p, \qquad \dot{d} = \dot{d}_e + \dot{d}_p. \tag{7}$$

For the plastic parts $\dot{\gamma}_p$ and $\dot{d}_p$ we have made the following constitutive assumptions:

$$\dot{\gamma}_p = \Lambda s, \qquad \dot{d}_p = \frac{\Lambda\sigma}{l}. \tag{8}$$

Λ in these equations equals zero whenever the deformations are elastic and is positive for plastic deformations. In order to determine whether a material point is deforming elastically or

plastically, we presume that a scalar loading or yield function f exists such that

$$f(s, \sigma, \theta, \dot{\gamma}_p, \dot{d}_p) = \kappa \tag{9}$$

and

$$\frac{\partial f}{\partial \Lambda}(s, \sigma, \theta, \Lambda s, \Lambda \sigma) < 0 \tag{10}$$

for all admissible values of s, σ and θ. κ in eqn (9) describes the work hardening of the material. The criterion for elastic and plastic deformation at a material point is

$$f(s, \sigma, \theta, 0, 0) \leq 0, \text{ elastic} \tag{11}$$

$$f(s, \sigma, \theta, 0, 0) > 0, \text{ plastic.} \tag{12}$$

When eqn (12) holds, eqn (9) has a unique solution for Λ because of the requirement (10). Equation (6) gives the value of Λ for the choices

$$f(s, \sigma, \theta, \dot{\gamma}_p, \dot{d}_p) = \frac{(s^2 + \sigma^2)^{\frac{1}{2}}}{(1 - a\theta)[1 + b(\dot{\gamma}_p^2 + \dot{d}_p^2)^{\frac{1}{2}}]^m}, \tag{13}$$

and

$$\kappa = \left(1 + \frac{\psi}{\psi_0}\right)^n. \tag{14}$$

The details of deriving eqns (1)–(6) may be found in Wright and Batra [9] and Green *et al.* [13].

The governing equations (1)–(6) are to be supplemented by initial conditions and boundary conditions. For the former we take

$$\begin{aligned} &v(y, 0) = y, \quad \theta(y, 0) = 0, \qquad \sigma(y, 0) = 0, \qquad \psi(y, 0) = 0, \\ &\theta(y, 0) = (1 + \cos 20\pi y)/20, \\ &s(y, 0) = [1 - a\theta(y, 0)], \end{aligned} \tag{15}$$

and for the latter

$$v(\pm 1, t) = \pm 1, \qquad \theta_{,y}(\pm 1, t) = 0, \qquad \sigma(\pm 1, t) = 0. \tag{16}$$

Thus the material point is initially presumed to lie on its yield surface that corresponds to quasistatic deformations, no work hardening and its initial temperature. The initial stress distribution is nonuniform and $\dot{\gamma}_p = 0$ initially at all points in the body.

We seek solutions of eqns (1)–(6) subjected to initial and boundary conditions (15) and (16) that exhibit the following symmetries and antisymmetries:

$$\begin{aligned} &v(-y, t) = -v(y, t), \qquad \theta(-y, t) = \theta(y, t), \\ &\sigma(-y, t) = -\sigma(y, t), \qquad s(-y, t) = s(y, t), \qquad \psi(-y, t) = \psi(y, t). \end{aligned} \tag{17}$$

However we do not assume *a priori* that the solution is periodic. Hence we can reduce the domain of study to $[0, 1]$ and replace boundary conditions (16) by

$$\begin{aligned} &v(1, t) = 1, \qquad v(0, t) = 0, \qquad \theta_{,y}(1, t) = 0, \qquad \theta_{,y}(0, t) = 0, \\ &\sigma(1, t) = 0, \qquad \sigma(0, t) = 0. \end{aligned} \tag{18}$$

The nonlinear coupled governing equations (1)–(5) under the side conditions (15) and (18) are solved numerically by the finite element method. We note that there are no existence and uniqueness theorems available for such a system of equations. Also there is no hope of solving these equations analytically, therefore we solve them numerically.

COMPUTATION AND DISCUSSION OF RESULTS

We introduce the auxiliary variables

$$u = v_{,y}, \qquad g = \theta_{,y}, \qquad p = \sigma_{,y} \tag{19}$$

and rewrite eqns (1)–(4) as

$$\dot{v} = \frac{1}{\rho}(s - lp)_{,y}, \tag{20}$$

$$\dot{\theta} = kg_{,y} + \Lambda(s^2 + \sigma^2), \tag{21}$$

$$\dot{s} = \mu(u - \Lambda s), \tag{22}$$

$$\dot{\sigma} = l\mu\left(u_{,y} - \frac{\Lambda}{l}\sigma\right). \tag{23}$$

Whereas Batra [11] integrated eqns (19)–(23) and (5) by the Crank–Nicholson–Galerkin finite element method to find u, g, p, v, θ, s, σ and ψ at a node point, we have integrated eqns (1)–(5) by the same method and computed v, θ, s, σ and ψ at a node point. For a test problem, the computed results by the two methods were identical but the core storage needed and the CPU time used was considerably less with the present method. Here we divided the domain $[0, 1]$ into 400 uniform subdomains or finite elements and used $\Delta t = 5 \times 10^{-6}$ in computing the results.

The values of the nondimensional parameters a, μ, n, ψ_0 and m do not depend upon the applied average strain-rate $\dot{\gamma}_0$ but those of ρ, k and b vary as $\dot{\gamma}_0^2$, $\dot{\gamma}_0^{-1}$ and $\dot{\gamma}_0$ respectively. The values of these variables, which correspond to a typical hard steel, used to compute numerical results are

$$a = 0.4973, \qquad \mu = 240.3, \qquad n = 0.09, \qquad \psi_0 = 0{\cdot}017, \qquad m = 0.025$$

and

$$\rho = 3.928 \times 10^{-5}, \qquad k = 3.978 \times 10^{-3}, \qquad b = 5 \times 10^{6} \text{ when } \dot{\gamma}_0 = 500\ \text{s}^{-1},$$

$$\rho = 3.928 \times 10^{-1}, \qquad k = 3.978 \times 10^{-5}, \qquad b = 5 \times 10^{8} \text{ when } \dot{\gamma}_0 = 50{,}000\ \text{s}^{-1}.$$

The presumed value of the thermal softening coefficient a is approx. 7 times the value for a typical steel. This is done so that the peak in the shear stress–shear strain curve occurs at a lower value of the average strain and therefore the computational time for the problem is significantly reduced. This choice of the value of a should not affect the qualitative nature of results presented here.

For homogeneous deformations of the block Fig. 1 depicts the shear stress–shear strain curve for an applied strain-rate of $500\ \text{s}^{-1}$. The peak in the curve occurs at an average strain of 0.093. At the higher strain-rate of $50{,}000\ \text{s}^{-1}$ the shear stress peaks out at an average strain of 0.085. The temperature perturbation was introduced at an average strain corresponding to point I in Fig. 1.

Figure 2 shows how the temperature, plastic strain-rate and the shear stress s evolve in the steel block when it is modeled as a nonpolar material, the initial temperature distribution is nonuniform, and the block is deformed at an average strain-rate of $500\ \text{s}^{-1}$. Figure 3 depicts the corresponding results for an applied strain-rate of $50{,}000\ \text{s}^{-1}$. Note that the initial temperature has the relative maximum value of 0.10 at $y = 0.0$, 0.1, 0.2, 0.3, 0.4, 0.5, 0.6, 0.7, 0.8, 0.9 and 1.0. In each case the shear stress s becomes essentially uniform after a short while and stays uniform throughout the thickness of the block. It first rises because of the work hardening and strain-rate hardening effects and begins to decrease when these hardening effects are overcome by the thermal softening. At the lower strain-rate of $500\ \text{s}^{-1}$ there is no noticeable drop in the shear stress even when the deformation has started to localize but at the higher strain-rate of $50{,}000\ \text{s}^{-1}$ the shear stress s decreases considerably after the deformation begins to localize.

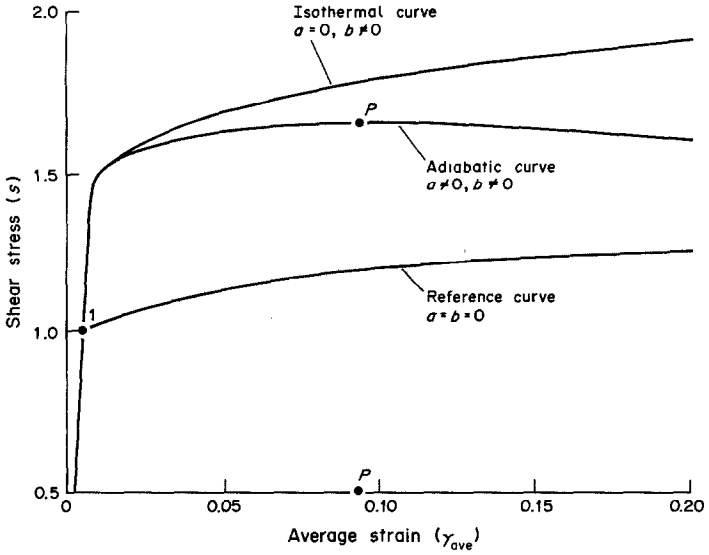

Fig. 1. Shear stress-strain curve for simple shearing deformations of a steel block at $\dot{\gamma}_0 = 500\,s^{-1}$.

This rather noticeable drop in the shear stress with increasing average strain after the deformation begins to localize has been pointed out by Wright and Walter [10]. Note that the temperature rise in the two cases at places where the deformation localizes is nearly equal to each other at the instant of the onset of the localization process. However, the temperature is more evenly distributed at $\dot{\gamma}_0 = 500\,s^{-1}$ as compared to that at $\dot{\gamma}_0 = 50{,}000\,s^{-1}$ in the sense that the difference between the maximum and the minimum temperature stays small for $\dot{\gamma}_0 = 500\,s^{-1}$ even after the deformation localizes. The rate of growth of the plastic strain-rate is more gradual at $\dot{\gamma}_0 = 500\,s^{-1}$ as compared to that at $\dot{\gamma}_0 = 50{,}000\,s^{-1}$.

The striking differences between the two cases are outlined below.

(a) First is the average strain at the instant the deformation begins to localize. For $\dot{\gamma}_0 = 500\,s^{-1}$ the average strain of 0.624 at which the deformation has essentially localized is nearly 7 times the strain at which the peak stress occurs during homogeneous deformations of the block. However, for $\dot{\gamma}_0 = 50{,}000\,s^{-1}$ the localization of the deformation occurs at an average strain of 0.09 which almost equals the strain of 0.085 at which the shear stress attains the maximum value during homogeneous deformations of the block. For comparison purposes we note [14] that when a temperature perturbation with a single bump centered at $y = 0$ is introduced, the shear bands form at an average strain of 0.0814 and 0.206 for $\dot{\gamma}_0 = 500\,s^{-1}$ and $50{,}000\,s^{-1}$, respectively. On the hypothesis that a temperature perturbation simulates material inhomogeneities or flaws in the body, the present results indicate the initiation of shear bands is delayed for $\dot{\gamma}_0 = 500\,s^{-1}$ when there are more defects uniformly distributed in the specimen, and for $\dot{\gamma}_0 = 50{,}000\,s^{-1}$ when there is only one defect present in the specimen.

(b) Secondly, the places where the peak temperature rise and the peak plastic strain-rate occur are quite different in the two cases. Whereas at $\dot{\gamma}_0 = 500\,s^{-1}$ the peak values of the temperature rise and the plastic strain-rate occur at places where the initial temperature perturbation had relative minimum values, at $\dot{\gamma}_0 = 50{,}000\,s^{-1}$ the peaks of the temperature rise and the plastic strain-rate coincide with the locations of the maxima of the temperature perturbation. That the centers of shear bands for $\dot{\gamma}_0 = 50{,}000\,s^{-1}$ coincide with the locations of the maxima of the initial temperature perturbation was also observed in the case the initial temperature perturbation assumed peak values at six equidistant points rather than eleven. In this case, the deformation localized at an average strain of 0.1122.

In order to understand the reasons for the above differences we note that, for nonpolar materials (i.e. $l = 0$), imbedded in the governing equations (1)–(6) are three length scales [9, 12] namely, the geometric length, a thermal length and a viscous length, and seven non-dimensional parameters, namely, the mass density ρ, the elastic modulus μ, the rate of

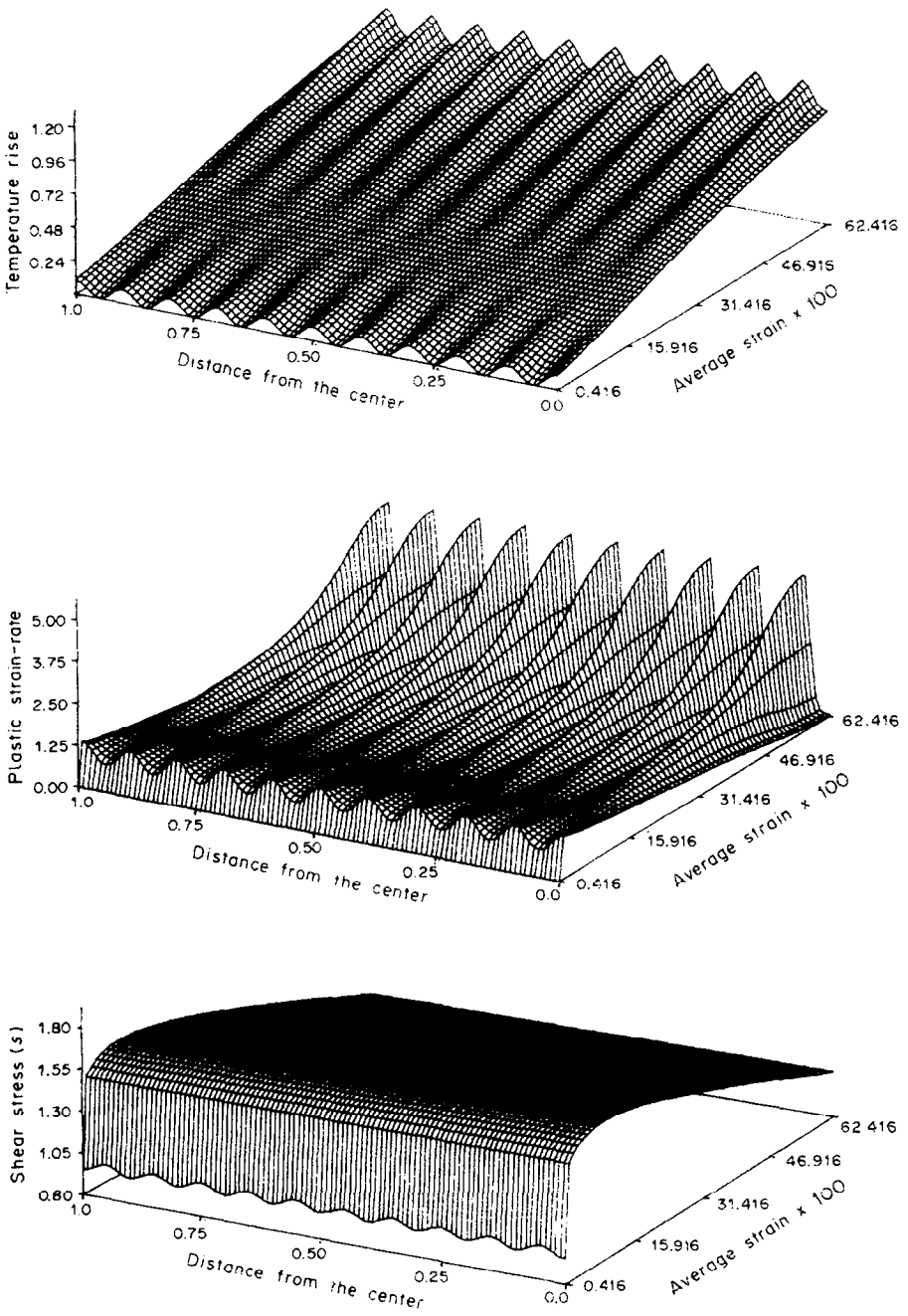

Fig. 2. Evolution of the temperature, plastic strain-rate and the shearing stress in nonpolar materials at $\dot{\gamma}_0 = 500\,s^{-1}$.

thermal softening a, two for work hardening n and ψ_0, and two for rate hardening b and m. Whereas the thermal length varies as $\dot{\gamma}_0^{-1/2}$, the viscous length does not depend upon $\dot{\gamma}_0$ but is a function of the material parameters. The non-dimensional thermal length (= thermal length/height of the specimen) is reduced from 0.6307 to 0.006307 when $\dot{\gamma}_0$ is increased from 500 to 50,000 s^{-1}. That the decrease in the thermal length is among the factors responsible for the aforementioned differences was confirmed by running the $\dot{\gamma}_0 = 500\,s^{-1}$ case with the thermal conductivity arbitrarily set equal to zero. In this case the thermal length is zero and the peak strain-rates occurred at the locations of the maxima of the initial perturbation as expected. To seek an answer to the question "For what value of $\dot{\gamma}_0$ does the above referred transition occur?", we conducted numerical experiments for different values of $\dot{\gamma}_0$ between 500

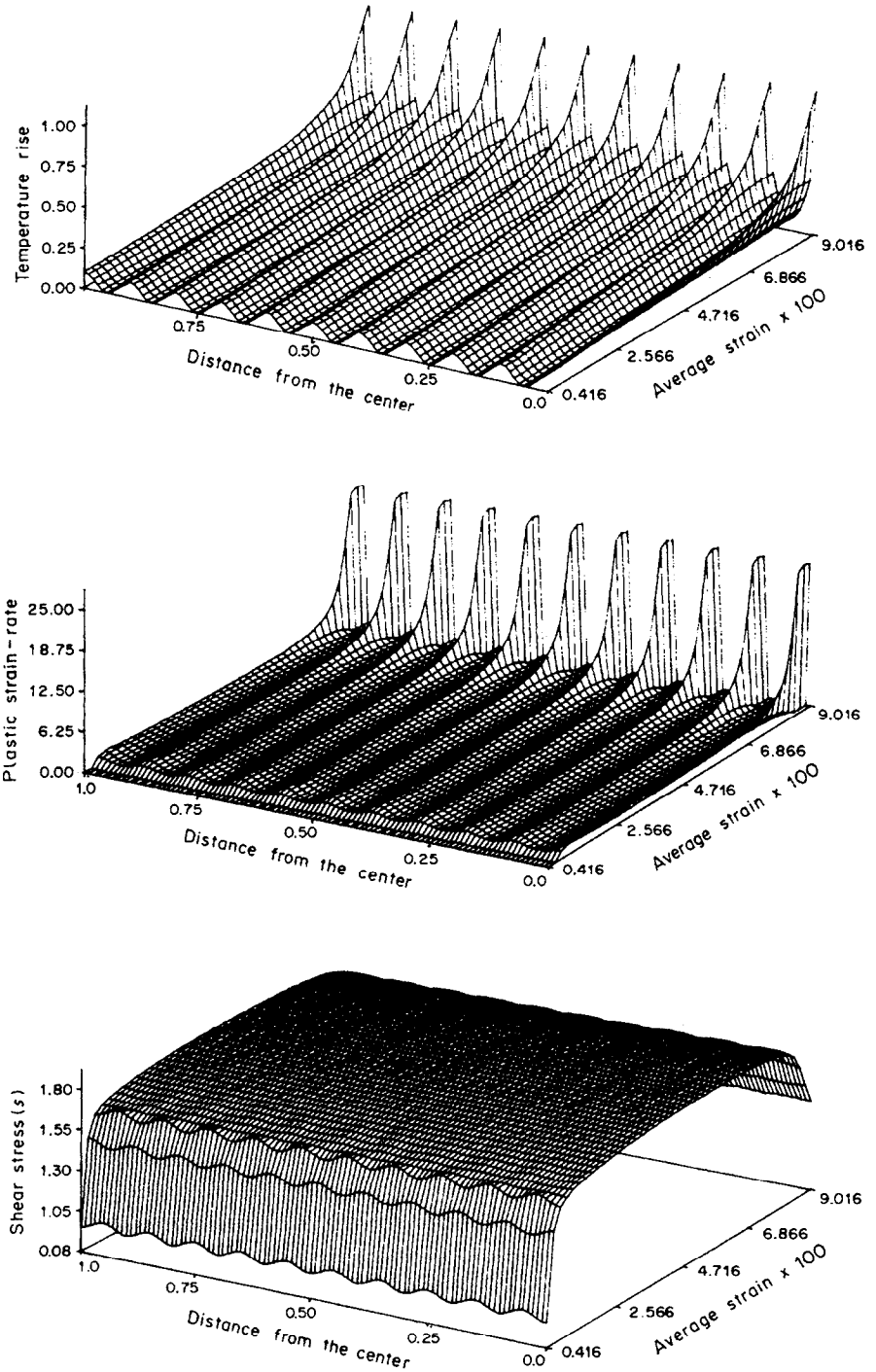

Fig. 3. Evolution of the temperature, plastic strain-rate and the shear stress in nonpolar materials at $\dot{\gamma}_0 = 50{,}000\,s^{-1}$.

and $50{,}000\,s^{-1}$ and found $\dot{\gamma}_0 = 1000\,s^{-1}$ to be the critical strain-rate above which the deformation localized at points of maxima of the initial temperature perturbation and below which it localized at other points.

It appears that it is the higher value of the thermal length at $\dot{\gamma}_0 = 500\,s^{-1}$ that delays the initiation of the localization process too. A close examination of the computed results indicated that initially the material points at the locations of the temperature maxima experienced peak plastic strain-rates and higher values of the work hardening parameter ψ as compared to their

neighbors. Since the shear stress became essentially uniform shortly after the temperature perturbation was introduced, the increased value of ψ resulted in reduced values of Λ, $\dot{\gamma}_p$ and the heat generated due to plastic working at these points. This coupled with the heat conduction tended to make the temperature virtually uniform throughout the specimen. Of course the temperature and work-hardening parameter did not become exactly uniform because if they did, the specimen will subsequently undergo homogeneous deformations only. To lend credence to this hypothesis we increased artificially the thermal conductivity to 100 times its previous value but kept $\dot{\gamma}_0 = 500\,s^{-1}$. In this case no shear band formed and the temperature field within the specimen became uniform and stayed so during the ensuing deformations. To understand the role played by the work-hardening, we conducted a numerical experiment with $n = 0$ and $\dot{\gamma}_0 = 500\,s^{-1}$. This resulted in neglecting the effect of the work-hardening on the deformations of the block. In this case the deformation localized at points where the initial temperature perturbation assumed peak values.

Another reason for the localization not to occur at the locations of the peaks in the initial temperature could be improper choices of the mesh and Δt. We reduced Δt to one-half of its value, but used the same mesh and recomputed results for $\dot{\gamma}_0 = 500\,s^{-1}$. For smaller time step the deformation localized at the same points as it did earlier for the large time step.

Since the distance between the locations of the points where the plastic strain-rate eventually peaked and points of maxima of the initial temperature perturbation equals approximately the length of 20 elements, it is unlikely that the finite-element mesh caused the shift.

When $\dot{\gamma}_0$ is increased from 500 to $50{,}000\,s^{-1}$, the non-dimensional mass density increases from 3.93×10^{-5} to 3.93×10^{-1}. In [14] the initial temperature perturbation had only one bump centered at $y = 0$. It was found that the shear stress distribution within the specimen was uniform for $\dot{\gamma}_0 = 500\,s^{-1}$ but non-uniform with the lowest value at $y = 0$ for $\dot{\gamma}_0 = 50{,}000\,s^{-1}$. No such non-uniformity in the shear stress distribution has been observed for the periodic initial temperature perturbation introduced herein.

In Figs 4 and 5 are plotted the evolution of the temperature, plastic strain-rate and the shear stress s when the material of the block is modeled as a dipolar material with $l = 0.01$ and the block is deformed at an average strain-rate $\dot{\gamma}_0$ of 500 and $50{,}000\,s^{-1}$ respectively. Whereas for $\dot{\gamma}_0 = 500\,s^{-1}$ only one shear band with center at $y = 1.0$ forms, at $\dot{\gamma}_0 = 50{,}000\,s^{-1}$ the deformation localizes around the location of the peaks of the initial temperature. In each case the initiation of the localization of the deformation is delayed as compared to that for nonpolar materials [14]; the delay is more pronounced at the higher applied strain-rate. Whereas for nonpolar materials the average strain at which the deformation localizes for $\dot{\gamma}_0 = 500\,s^{-1}$ is nearly seven times that for $\dot{\gamma}_0 = 50{,}000\,s^{-1}$, for dipolar materials the average strains at which the deformation localizes in the two cases are nearly equal to each other. Also for nonpolar materials the shear stress s becomes essentially uniform throughout the specimen soon after the initial perturbation is introduced and stays uniform within the block, such is not the case for dipolar materials. For dipolar materials the amplitude of the oscillations in the shear stress distribution is extremely small for $\dot{\gamma}_0 = 500\,s^{-1}$ but at $\dot{\gamma}_0 = 50{,}000\,s^{-1}$ it is noticeable and seems to grow as the deformation localizes. Note that for dipolar materials it is $(s - l\sigma_{,y})$ and not s that acts as a flux for the linear momentum. The average shear stress s exhibits the same behavior as that for nonpolar materials in the sense that it first increases and subsequently begins to drop when thermal softening effects exceed the combined effects of strain and strain-rate hardening.

At $\dot{\gamma}_0 = 500\,s^{-1}$ the initial temperature distribution tends to become uniform throughout the block and stays virtually uniform until the deformation begins to localize near $y = 1.0$. At that instant the temperature near $y = 1.0$ increases slightly more than that at other places. Of course the temperature at every point in the body keeps on increasing because of the plastic working. Why the shear band forms near $y = 1.0$ and not near $y = 0.0$ is not clear. At the higher applied strain-rate $\dot{\gamma}_0 = 50{,}000\,s^{-1}$ neither the temperature nor the plastic strain-rate ever becomes uniform within the block. It seems that the amplitude of the temperature oscillations keeps on increasing with the increase in the average strain in the specimen.

For dipolar materials, in addition to the thermal and viscous lengths, there are three length scales [13] characteristic of the material. Herein as well as in two previous studies [9, 11] the

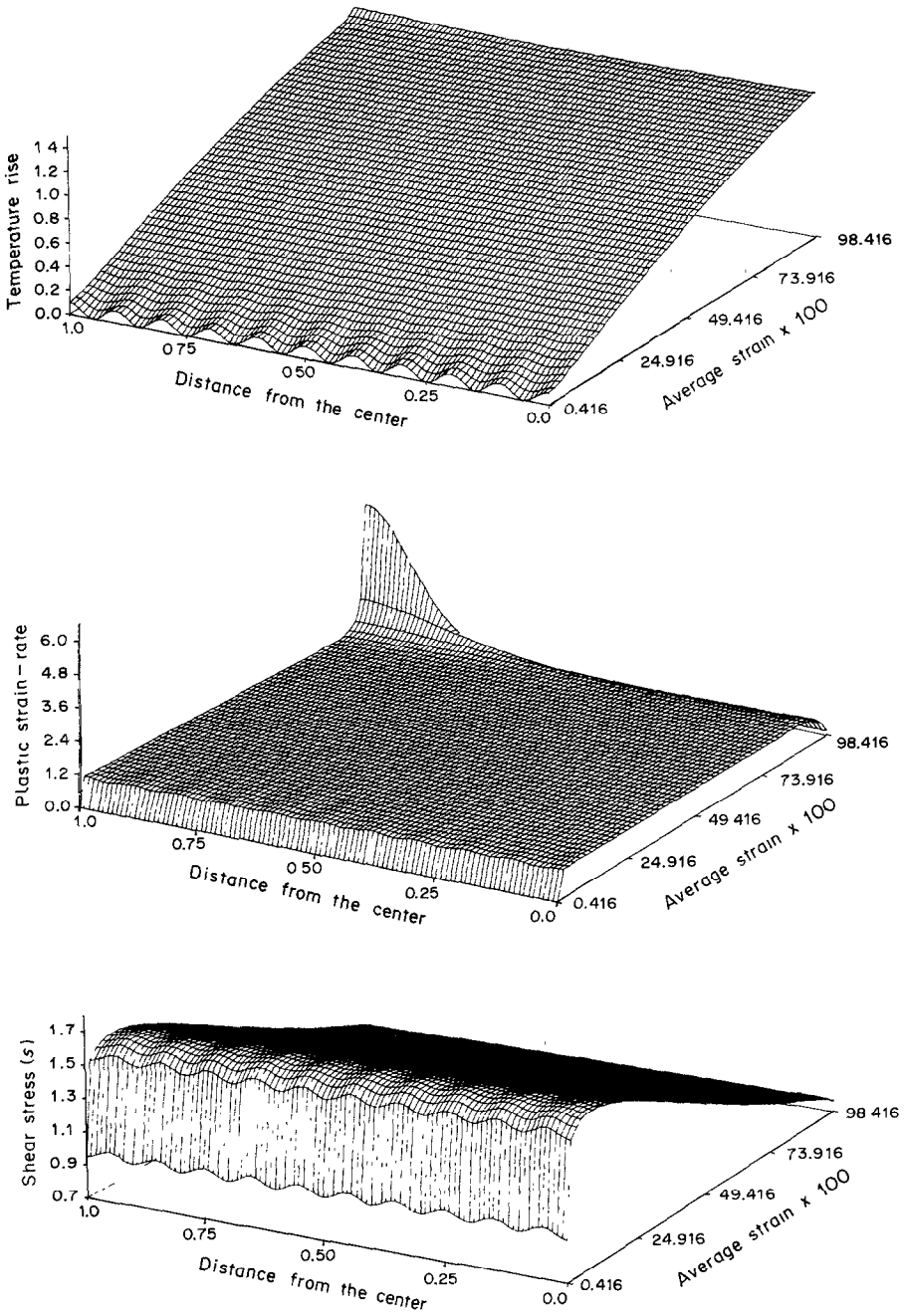

Fig. 4. Evolution of the temperature, plastic strain-rate and the shear stress in dipolar materials ($l = 0.01$) at $\dot{\gamma}_0 = 500\,s^{-1}$.

three length scales have been set equal to each other. The problem when the three length scales are different is under investigation and will be reported on in a future paper. The previous work with $\dot{\gamma}_0 = 500\,s^{-1}$ and with a single temperature perturbation centered at $y = 0$ indicated that the inclusion of dipolar effects delays considerably the localization of the deformation. The delay observed here by comparing results plotted in Figs 3 and 5 is significantly more as compared to that found previously and also that computed presently for $\dot{\gamma}_0 = 50{,}000\,s^{-1}$. The main reason for the difference between the previously computed [9, 11] and current results is due to the number of flaws/imperfections considered in the two cases. An explanation for the difference between the results computed at $\dot{\gamma}_0 = 500$ and $50{,}000\,s^{-1}$ lies in the different values of the thermal lengths in the two cases. At $\dot{\gamma}_0 = 500\,s^{-1}$ the temperature

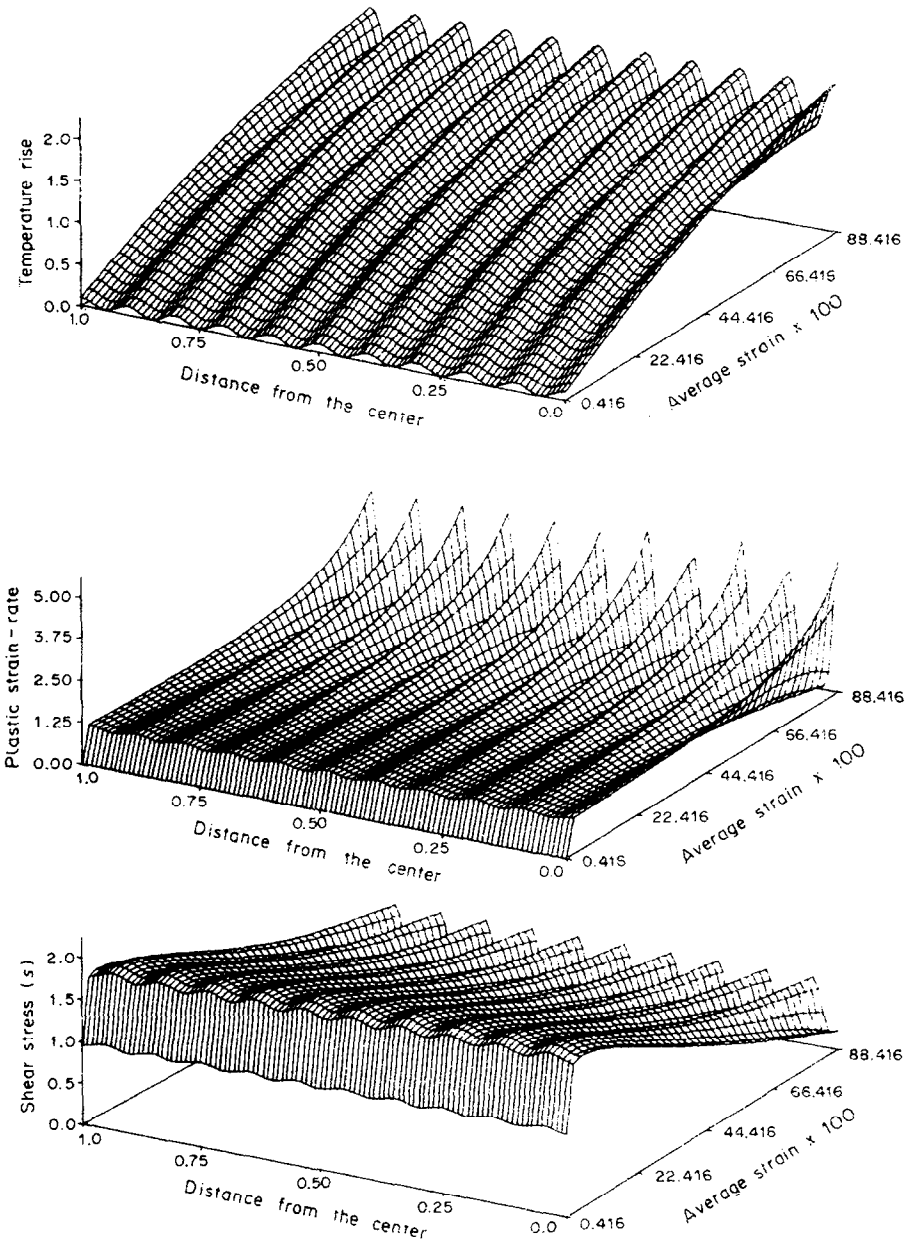

Fig. 5. Evolution of the temperature, plastic strain-rate and the shear stress in dipolar materials ($l = 0.01$) at $\dot{\gamma}_0 = 50{,}000\,s^{-1}$.

initially tends to become uniform because of heat conduction and once the temperature fluctuations die out the block deforms homogeneously. What eventually causes the temperature to rise at $y = 1.0$ and not at $y = 0.0$ is unclear.

We note that the CPU time required to compute results for the dipolar materials is nearly four times that needed for non-polar materials. Thus not many numerical experiments could be conducted for dipolar materials.

CONCLUSIONS

For nonpolar materials the initiation of the shear bands is significantly delayed at $\dot{\gamma}_0 = 500\,s^{-1}$ when a periodic temperature perturbation with eleven peaks is introduced initially as compared to the case when the initial temperature perturbation has a single bump with peak at the center

of the block. However, for $\dot{\gamma}_0 = 50{,}000\,s^{-1}$ the reverse happens. In the former case the deformation localizes at points where the initial temperature has relative minima values, in the latter case the centers of shear bands coincide with the places where the initial temperature has relative maximum values. These transitions are found to occur at $\dot{\gamma}_0 = 1000\,s^{-1}$ and seem to be caused by the lower value of the thermal length at the higher value of $\dot{\gamma}_0$ and the different time scale associated with the work-hardening in the two cases.

For dipolar materials the average strains in the specimen at which the deformation localizes at $\dot{\gamma}_0 = 500$ and $50{,}000\,s^{-1}$ are nearly equal to each other. These values of average strains are higher than the corresponding values for nonpolar materials. Only one band forms at $\dot{\gamma}_0 = 500\,s^{-1}$ but the number of shear bands equal the number of peaks in the initial temperature at $\dot{\gamma}_0 = 50{,}000\,s^{-1}$.

Acknowledgements—This work was partially supported by the U.S. Army Research Office Contract DAAG29-85-K-0238 and the U.S. NSF grant MSM-8715952 to the University of Missouri-Rolla. We are indebted to Dr T. W. Wright and John Walter for useful discussions on the subject.

REFERENCES

[1] R. F. RECHT, *ASME J. appl. Mech.* **31,** 189 (1964).
[2] M. R. STAKER, *Acta metall.* **29,** 683 (1981).
[3] R. J. CLIFTON, NRC National Material Advisory Board (U.S.) Report 356 (1980).
[4] T. J. BURNS, *Q. Jl appl. Math.* **43,** 65 (1985).
[5] Y. L. BAI, in *Shock Waves and High Strain Rate Phenomenon in Metals* (Edited by M. A. MEYERS and L. E. MURR), p. 277. Plenum Press, New York (1981).
[6] T. G. SHAWKI, R. J. CLIFTON and G. MAJDA, ARO Report DAAG 29-81-K-0121/3, Brown University (1983).
[7] R. J. CLIFTON, J. DUFFY, K. A. HARTLEY and T. G. SHAWKI, *Scripta metall* **18,** 43 (1984).
[8] T. W. WRIGHT and R. C. BATRA, *Int. J. Plasticity* **1,** 205 (1985).
[9] T. W. WRIGHT and R. C. BATRA, in *Proc. IUTAM Symposium on Macro- and Micromechanics of High Velocity Deformation and Fracture* (Edited by K. KAWATA and J. SHIOIRI), p. 189, Springer, Berlin (1987).
[10] T. W. WRIGHT and J. W. WALTER, *J. Mech. Phys. Solids.* **35,** 701 (1987).
[11] R. C. BATRA, *Int. J. Plasticity* **3,** 75 (1987).
[12] R. C. BATRA, *Int. J. Solids Struct.* **23,** 1435 (1987).
[13] A. E. GREEN, B. C. McINNIS, and P. M. NAGHDI, *Int. J. Engng Sci.* **6,** 373 (1968).
[14] R. C. BATRA, *ASME J. appl. Mech.* **55,** 229 (1988).

(*Revised version received* 2 *March* 1988)